water

MDPI

Article

Afforestation of Degraded Croplands as a Water-Saving Option in Irrigated Region of the Aral Sea Basin

Navneet Kumar [1], Asia Khamzina [2,*], Patrick Knöfel [3], John P. A. Lamers [1] and Bernhard Tischbein [1]

[1] Center for Development Research (ZEF), University of Bonn, Genscherallee 3, 53113 Bonn, Germany; nkumar@uni-bonn.de (N.K.); jlamers@uni-bonn.de (J.P.A.L.); tischbein@uni-bonn.de (B.T.)

[2] Division of Environmental Science and Ecological Engineering, Korea University, 145 Anam-Ro, Seongbuk-Gu, Seoul 02841, Korea

[3] Department of Remote Sensing, University of Würzburg, Oswald-Külpe-Weg 86, 97074 Würzburg, Germany; patrick.knoefel@bkg.bund.de

* Correspondence: asia_khamzina@korea.ac.kr

Abstract: Climate change is likely to decrease surface water availability in Central Asia, thereby necessitating land use adaptations in irrigated regions. The introduction of trees to marginally productive croplands with shallow groundwater was suggested for irrigation water-saving and improving the land's productivity. Considering the possible trade-offs with water availability in large-scale afforestation, our study predicted the impacts on water balance components in the lower reaches of the Amudarya River to facilitate afforestation planning using the Soil and Water Assessment Tool (SWAT). The land-use scenarios used for modeling analysis considered the afforestation of 62% and 100% of marginally productive croplands under average and low irrigation water supply identified from historical land-use maps. The results indicate a dramatic decrease in the examined water balance components in all afforestation scenarios based largely on the reduced irrigation demand of trees compared to the main crops. Specifically, replacing current crops (mostly cotton) with trees on all marginal land (approximately 663 km^2) in the study region with an average water availability would save 1037 mln m^3 of gross irrigation input within the study region and lower the annual drainage discharge by 504 mln m^3. These effects have a considerable potential to support irrigation water management and enhance drainage functions in adapting to future water supply limitations.

Keywords: drainage ratio; irrigation; spatial water balance; Soil and Water Assessment Tool (SWAT); scenario analysis; stream flow; water yield

Citation: Kumar, N.; Khamzina, A.; Knöfel, P.; Lamers, J.P.A.; Tischbein, B. Afforestation of Degraded Croplands as a Water-Saving Option in Irrigated Region of the Aral Sea Basin. *Water* **2021**, *13*, 1433. https://doi.org/10.3390/w13101433

Academic Editor: Pilar Montesinos

Received: 5 April 2021
Accepted: 18 May 2021
Published: 20 May 2021

1. Introduction

Climate change predictions for Central Asia point to a probable increase in atmospheric temperature coupled with a decrease in precipitation [1], which stipulate an increase in annual evapotranspiration [2]. These changes are likely to reduce crop yields by as much as 30% and cause substantial economic losses in this region, which is highly dependent on irrigated agriculture [3]. Irrigated agriculture in Central Asia annually utilizes approximately 90% of the 120 km^3 of water in the catchments of the Amudarya and Syrdarya rivers [4], while water management remains notoriously inefficient, characterized by excessive irrigation, associated water losses, and rising groundwater tables [5,6]. The other major concern that is likely to worsen owing to climate change is cropland degradation and yield declines resulting from soil salinization. The latter is rampant in the downstream countries, affecting approximately 50% of irrigated land in Uzbekistan and 95% in Turkmenistan [7–9].

Under the decreasing availability of freshwater for land reclamation via salt leaching, cropping operations in highly salinized areas in the Amudarya downstream are being abandoned [10,11]. Converting degraded cropland parcels to carbon-dense systems of salt-tolerant tree species, as examined at field and farm scales, can improve the soil fertility and productivity of degraded croplands [12] by generating non-timber and timber products of commercial value and contributing to carbon sequestration efforts [13]. Areas experiencing elevated groundwater tables are particularly promising for tree planting because of the possibility of reducing the irrigation water demand for afforested areas [14,15]. Experiences in drylands elsewhere emphasize the role of tree plantations as a low-cost measure in improving salt balances by controlling elevated water tables in agricultural regions at both the farm and regional scales [16,17].

However, as trees are substantial water consumers, larger-scale afforestation efforts in drylands may lead to negative hydrological impacts [18–20], including critical declines in groundwater tables, the depletion of soil water, and reduced annual runoff and water yields [21–23]. Among the types of land use conversion to forestry, the afforestation of grassland and shrubland has been most often associated with a reduction in the annual runoff, especially when using tree species that demonstrate profligate water use [23,24]. The adverse hydrological outcomes of planting trees can introduce considerable trade-offs with recognized benefits and reduce the appeal for tree planting, thereby requiring an ex ante assessment and planning of afforestation. Especially with a decreasing surface water supply and the cropland degradation experienced in Central Asia, the potential impact of afforestation on the water balance must be understood beyond the field scale, and tree planting interventions should be aligned with the water availability in the landscape [15].

Previous studies in the Amudarya downstream considered the surface water supply [11] or spatially variable water supply-demand [15] in assessments of site suitability for afforestation. A further evaluation of the hydrological impacts of tree planting requires approaches and tools capable of capturing complex temporal and spatial dynamics of the climate–forest–water nexus. Hydrological models offer many possibilities within this context, as they represent the processes in the hydrological system to quantify water fluxes and balances covering either the full hydrological cycle or part of it. Distributed hydrological models estimate the water flow directly from the governing partial differential equations and consider the spatial and temporal behaviors of the variables, and hence, are increasingly reflective of reality [25]. Various hydrological models have been employed to investigate the impacts of land use, land cover, and climate change on water resources. These hydrological models such as Hydrologiska Byråns Vattenbalansavdelning (HBV) [26], MIKE-Système Hydrologique Européen (MIKE-SHE) [27,28], Water Flow and Balance Simulation Model (WaSiM) [29,30], Variable Infiltration Capacity (VIC) [31], and the Soil and Water Assessment Tool (SWAT) [32,33] among others, have been useful in analyzing past as well as future impacts. Among these models, SWAT is known for its multi-objective applications, including impact analyses of forest cover dynamics on water balance components [34–36] and integrating multiple environmental processes and watershed management practices to provide an informational base for policy decisions [37]. A plethora of studies have used SWAT-based applications in assessments of the impacts of climate and land use changes on hydrological processes and water balance components under different environmental conditions worldwide [32,38].

Our study used the SWAT hydrological model to analyze the potential impacts of tree plantations on water balance components based on relevant scenarios reflecting the spatial and temporal variability of land use and irrigation water availability in the lower Amudarya River region. We hypothesize that the conversion of degraded croplands to tree plantations will bring a favorable decrease in irrigation water use, but the associated hydrological impacts will depend on the scale of afforestation.

2. Materials and Methods

2.1. Study Area

The study region of Khorezm is located between 60.05° and 61.39° E and 41.13° and 42.02° N, bordering the Karakum and Kyzylkum deserts in the south, southwest, and west, and the Amudarya River in the northeast (Figure 1).

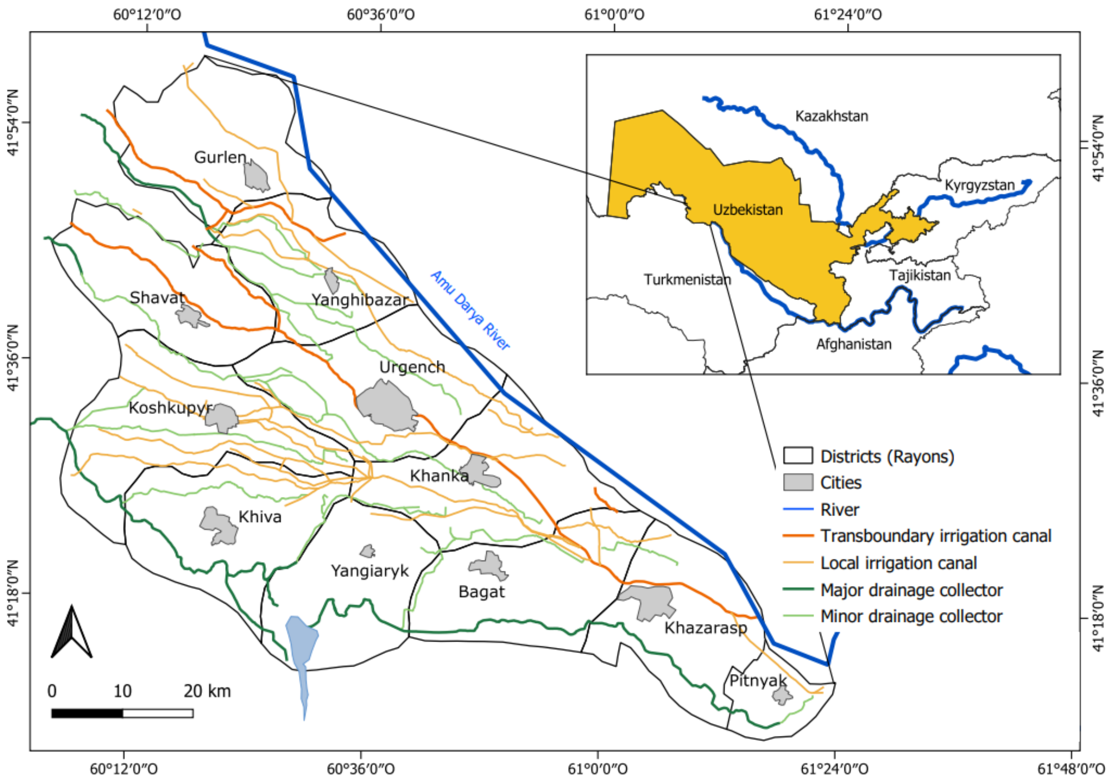

Figure 1. Location of the Khorezm region, as well as its main irrigation and drainage collector network in the lower Amudarya River Basin, Uzbekistan. Source: Khorezm Geographic Information System (GIS) laboratory.

The study area's average annual rainfall of 100 mm is greatly exceeded by evapotranspiration, having required the construction of an extensive canal and drain network for the irrigation of agricultural crops (Figure 1). Khorezm's location in the lower reaches in the regional topography is flat, with an elevation difference of 55 m a.s.l. toward the northwest (Figure 2). The hydraulic gradient is low, leading to a slow lateral groundwater flow and shallow groundwater conditions, which are exacerbated by irrigation and marginal functional drainage [5,39,40]. Given that surface runoff is prevented from irrigated fields, which are leveled and surrounded by bunds, the discharge in the drainage system is generated primarily from the groundwater recharged by irrigation and leaching water losses.

Rising groundwater levels have instigated ubiquitous secondary soil salinization that is treated with pre-seasonal salt leaching [5,41,42]. Despite these efforts, approximately 20% of the irrigated cropland area is characterized by marginal productivity [11] that affects the yields of major crops and the revenues of the regional economy [13].

2.2. SWAT Modeling

SWAT, developed by the Agricultural Research Service (ARS), United States Department of Agriculture (USDA), is a physically based, daily time step, river basin or watershed-scale, and a semi-distributed hydrological model that can be integrated with GIS. SWAT is freely available and has strong network support [32]. These characteristics have allowed SWAT modelers to effectively address the main challenges faced by hydrological models, such as deficient data, spatial heterogeneity, and complex processes in study catchments [37]. Nevertheless, SWAT has limited capabilities for groundwater modeling.

SWAT integrates the following main components: weather, surface runoff, return flow, percolation, evapotranspiration, transmission losses, pond and reservoir storage, crop growth and irrigation, groundwater flow, reach routing, nutrient and pesticide loading, and water transfers. The quantification of the hydrological cycle in the SWAT is based on the water balance equation:

$$SW_t = SW0 + \sum_{i=1}^{t}(Rday - Qsurf - Ea - Wseep - Qgw) \quad (1)$$

where SW_t = final soil water content (mm), $SW0$ = initial soil water content on day i (mm), $Rday$ = amount of precipitation on day i (mm), $Qsurf$ is the amount of surface runoff on day i (mm), Ea is the amount of evapotranspiration on day i (mm), $Wseep$ is the amount of water entering the vadose zone from the soil profile on day i (mm), and Qgw is the amount of return flow on day i (mm).

The basic principle behind SWAT modeling is a two-step partitioning of the study watershed into sub-units. First, topographic discretization is performed by dividing the watershed into several sub-basins that are used to determine the routing structure of water and pollutants throughout a spatially heterogeneous watershed. Second, the input information for each sub-basin is grouped into the following categories: climate, hydrological response units (HRUs), ponds/wetlands, groundwater, and the main channel or reach draining the sub-basin. The HRUs are obtained by overlaying the spatial data and are lumped areas within the sub-basin that comprise a unique combination of land cover, soil type, slope, and management practices.

For this study, the SWAT model was set up between 2000 and 2010 (11 years). The simulations were run with daily time steps, which were further aggregated to annual time steps. Spatial input data, including a digital elevation model (DEM), as well as climate, land use, and soil maps available in various spatial resolutions in a grid format or as point data, were processed and prepared in the SWAT-required format (Table S1). The irrigation amount, crop growth parameters, and crop rotation data were fed into the model (Figure 2).

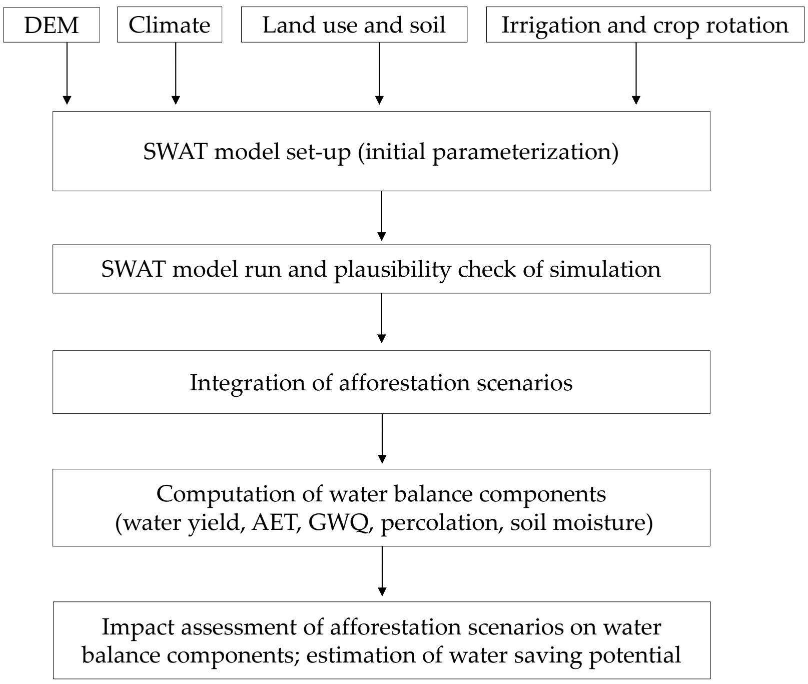

Figure 2. Methodology flowchart diagram.

Water balance components, including percolation, surface runoff, groundwater contribution to streamflow (GWQ), water yield, and actual evapotranspiration (AET) were computed using Equation (1). Using the DEM, drainage network, and river boundaries as inputs, SWAT delineated 107 sub-catchments and 6617 HRUs within the Khorezm catchment (Figure S1). No threshold was applied to generate HRUs.

The lack of ground-observed data on discharge in the drainage system precluded the calibration and validation of the SWAT model. However, the model was parameterized using the Khorezm region database and published research specific to the study region (Table S1). Plausibility checks for SWAT simulations were conducted by comparing the computed drainage ratio (the relation of simulated drainage output to the gross irrigation water supply plus precipitation) and the modeled values of water balance components with the published estimates relevant to Khorezm's irrigation and drainage system.

2.3. Data Description and Analysis

2.3.1. Digital Elevation Model (DEM) and Climate

The Shuttle Radar Topography Mission (SRTM) DEM with a resolution of 90 m (Figure 3) was downloaded from the Consultative Group on International Agricultural Research (CGIAR) Consortium website for spatial information on elevation [43].

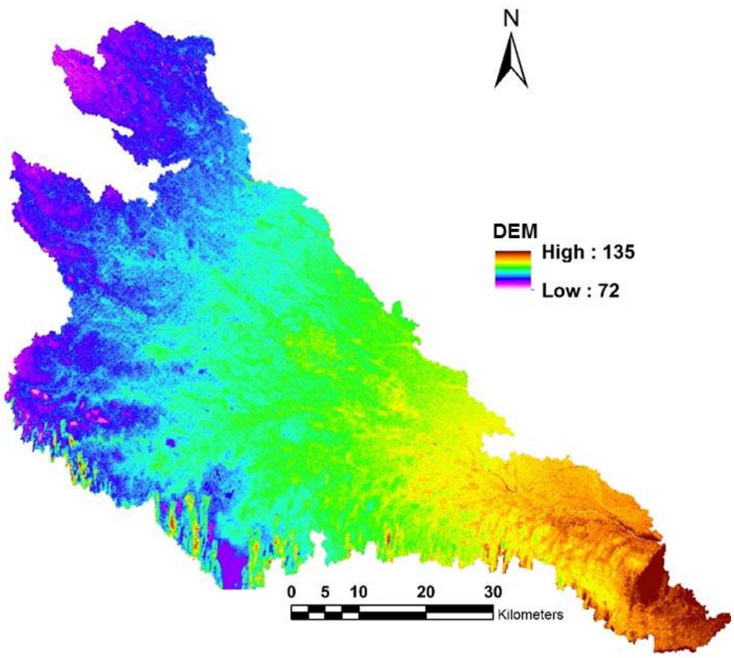

Figure 3. Digital Elevation Model (DEM) of the Khorezm region, Uzbekistan. Source: [43].

Data from five locations in Khorezm were processed to capture the spatial variability in rainfall in daily time steps for 2000–2010 as previously reported [15]. SWAT considers one meteorological value for each sub-basin based on the nearest location. The climate parameters were rainfall (mm), maximum and minimum air temperature (°C), relative humidity (%), wind speed (km h^{-1}), and sunshine duration (h). Sunshine hours were converted to solar radiation (MJ m^{-2}) using Cropwat 8.0. Source data were collected from the Khorezm region database [44,45].

The rainfall during the study period ranged from 54 to 167 mm, with an average of 99 mm (2000–2010). The average rainfall amount for 2005 and 2008 in Khorezm totaled 111 mm and 76 mm, respectively (Figure 4).

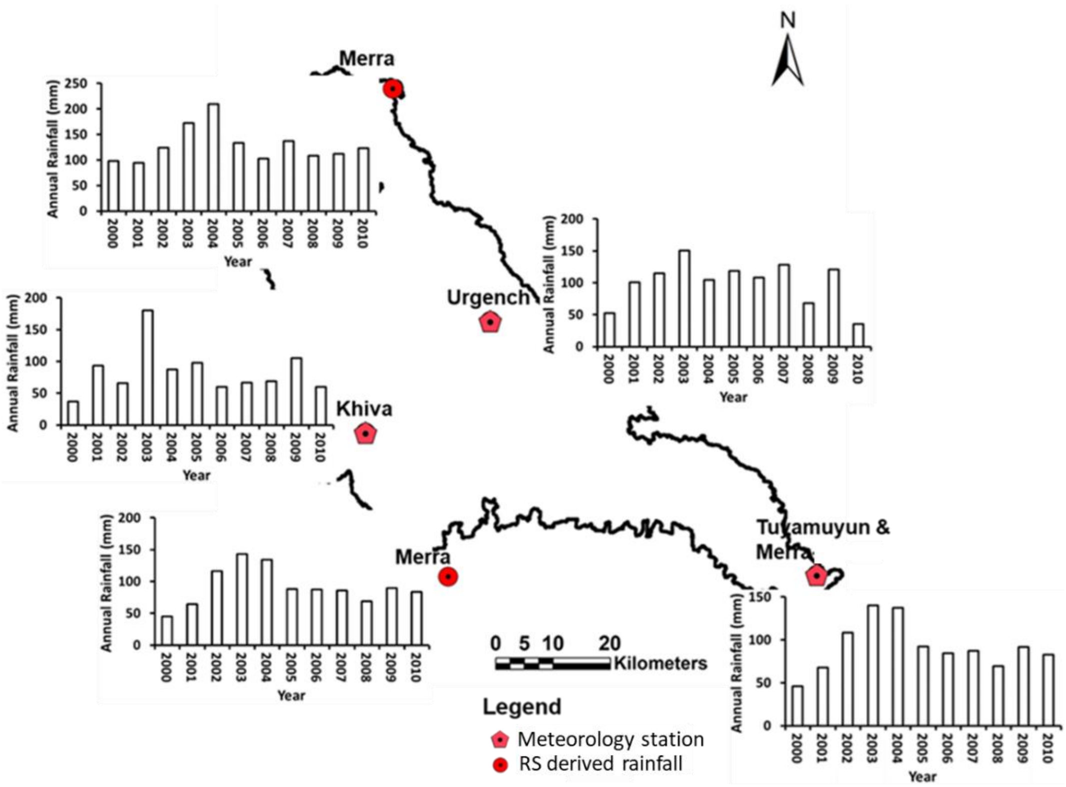

Figure 4. Locations of meteorological stations and the spatial distribution of annual precipitation during 2000–2010 as recorded by three stations and as estimated through remote sensing (RS) in the Khorezm region, Uzbekistan. Source: Reference [15].

2.3.2. Soil

Figure 5 shows soil types represented by 168 polygons, 43 soil types, and 1887 measured soil samples. This soil map, used as an input in the SWAT model, considers three soil layers (0–30 cm, 30–100 cm, and 100–150 cm), each with spatially interpolated information on soil parameters.

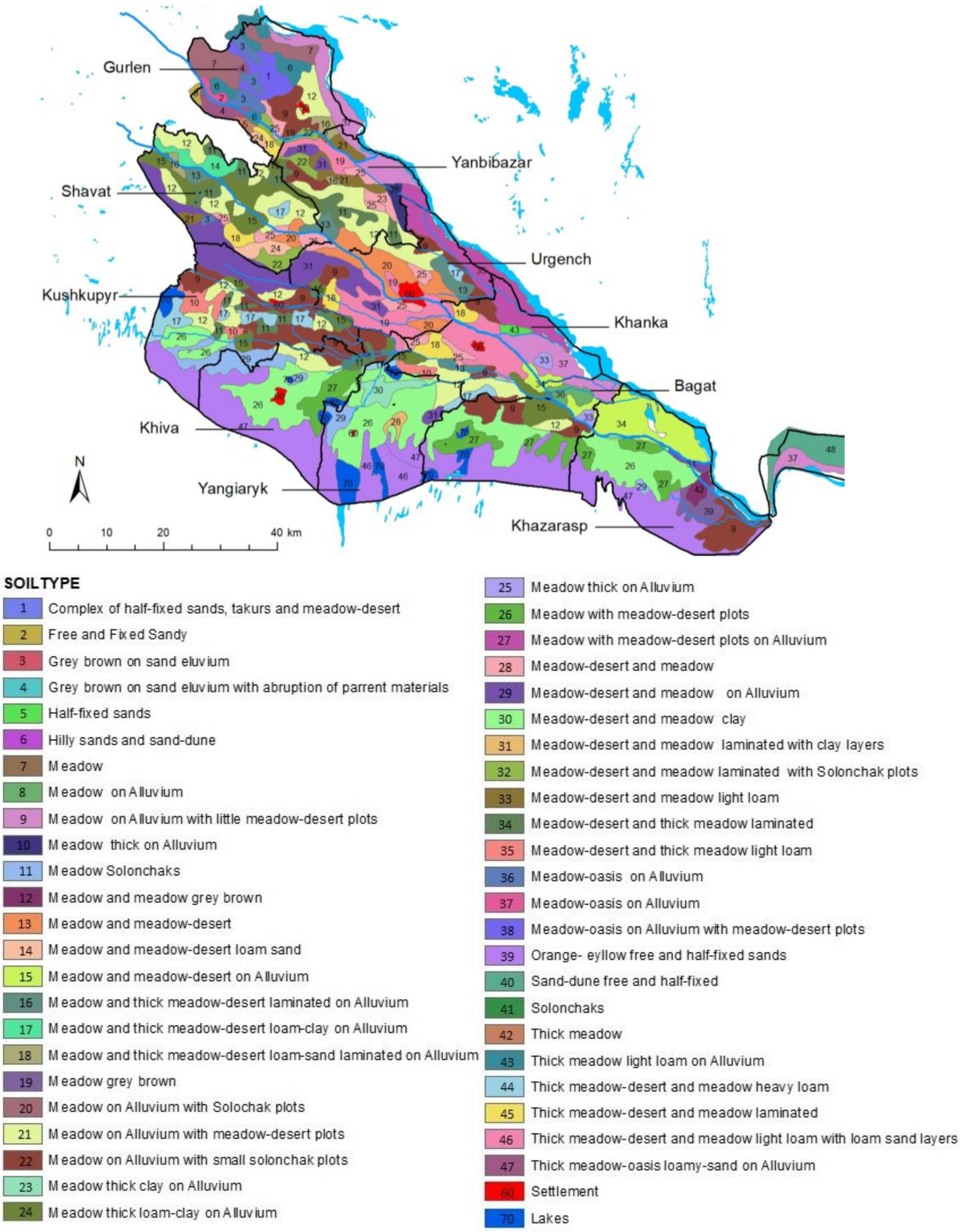

Figure 5. Soil types for the 0–150 cm profile shown for administrative districts of Khorezm, Uzbekistan (scale: 1:100,000). Source: [46].

The SWAT model setup of soil physical properties required 17 soil parameters for each polygon and soil layer (168 × 3 × 17 = 8568 attributes): soil name (optional), soil hydrologic group (A,B,C,D) based on the USDA classification [47], maximum rooting depth of soil profile (mm), fraction of porosity (void space) from which anions are excluded (optional), potential or maximum crack volume of the soil profile expressed as a fraction of the total soil volume (optional), texture of the soil layer (optional), depth from the soil surface to the bottom of a layer (mm), moist bulk density (g cm^{-3}), available water capacity of the soil layer (Field Capacity (FC)–Wiliting Point (WP), mm H_2O mm^{-1} soil), saturated hydraulic conductivity (Ks, mm h^{-1}), organic carbon content (% soil weight), clay content (% soil weight), silt content (% soil weight), sand content (% soil weight), rock fragment content (% total weight), moist soil albedo, and the USLE equation-based soil erodibility factor (K_{USLE}) (0.013 (metric ton m^2 h)/(m^3 metric ton cm)). Six of the required soil parameters were not available: soil bulk density, FC-WP, Ks, moist soil albedo, soil hydrologic group, and K_{USLE} (soil erodibility K factor for the top layer). These missing parameters were estimated using the Soil Par version 2.0 beta software. The Campbell method (retention function pedotransfer) was used to estimate Ks and FC-WP, and the Baumer method (point and function pedotransfer) was used to estimate the bulk density. Moist soil albedo values were extracted from the Moderate Resolution Imaging Spectroradiometer (MODIS) image (500 m spatial resolution) of 1 April 2010. The extracted values ranged from 0.064–0.28. K_{USLE} was estimated based on [48]:

$$K_{USLE} = fcsand \times fci - si \times forgc \times fhisand \quad (2)$$

where *f csand* is a factor that gives low soil erodibility factors for coarse (sandy) soils and vice versa; *f ci-si* is a factor that gives low soil erodibility factors for soils with high clay to silt ratios, *forgc* is a factor that reduces soil erodibility for soils with high organic carbon content, and *f hisand* is a factor that reduces soil erodibility for soils with extremely high sand content.

$$fcsand = 0.2 + 0.3 \times \exp\left[-0.256 \times ms \times \left(1 - \frac{msilt}{100}\right)\right] \quad (3)$$

$$fci - si = \left(\frac{msilt}{mc + msilt}\right)^{0.3} \quad (4)$$

$$f\ \mathrm{orgc} = \left(1 - \frac{0.0256 \times orgC}{orgC + \exp[3.72 - 2.95 \times orgC]}\right) \quad (5)$$

$$f\ hisand = 1 - \frac{0.7\left(1 - \frac{ms}{100}\right)}{\left(1 - \frac{ms}{100}\right) + \exp\left[-5.51 + 22.9\ \left(1 - \frac{ms}{100}\right)\right]} \quad (6)$$

where *ms* is the sand fraction percentage (0.05–2.00 mm diameter particles), *msilt* is the percentage of silt (0.002–0.05 mm diameter particles), *mc* is the percentage of clay (<0.002 mm diameter particles), and *orgc* is the organic carbon concentration of the layer (%).

2.3.3. Land Use

The land use statistics for SWAT modeling were derived using multi-temporal land use classification using satellite data [49]. The MODIS-based Normalized Difference Vegetation Index (NDVI) time series (geometric resolution of 250 m) for 2000–2010 was used in combination with a random forest model classification approach. A quality assessment was applied to the MODIS time series, and data affected by clouds or data production problems were linearly interpolated over time. The comparison of different satellite-based vegetation index products showed that the NDVI based on 8-day surface reflectance (MOD09Q1) was the most suitable for vegetation monitoring in Khorezm [49]. The land use maps contained three non-agricultural classes, namely settlements, water, and fallow (barren) land, and five agricultural land use types: cotton, rice, wheat-fallow, wheat-rice, and wheat-other crops (Figure 6).

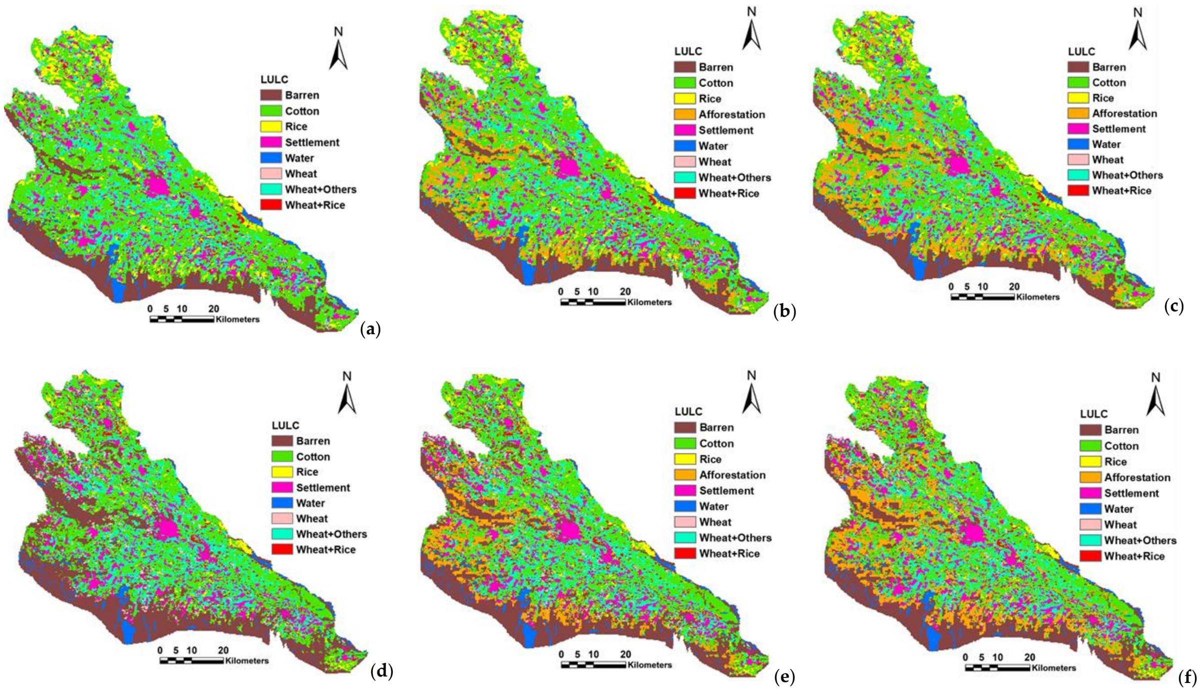

Figure 6. Land use map for 2005 representing average conditions (**a**), 62% afforestation (2005) (**b**), 100% afforestation (2005) (**c**), land use map 2008, representing drought conditions (**d**), 62% afforestation (2008) (**e**), and 100% afforestation (2008) (**f**). Source: [49].

The land use maps of 2005 and 2008 (Figure 6a,d, respectively) were used as a reference in the SWAT setup. The year 2005 was the midterm in the model simulation period (2000–2010) and represented the average water availability conditions. A land use map of 2008 was selected because it represents an agricultural drought year with reduced cropping area and irrigation amount as compared to the average. Cotton accounted for the largest share of arable land in all years, amounting to 44.6% in 2005. In 2008, the cotton share declined to 31.8%, and that of rice also decreased from 5.8% to 2.0%, whereas fallow areas increased from 13.2% to 27.3%. The percentage of the wheat-only class increased slightly from 1.4% to 3.4% because the reduced water supply in 2008 limited the cultivation of the second crop after wheat.

2.3.4. Irrigation

The surface water applications to different land use classes were estimated based on local standards for irrigation requirements depending on crop type (predominantly cotton, followed by rice, winter wheat, and crop rotations with winter wheat) and the prevalent hydro-module zone (Table 1; [15]).

Table 1. Crop water requirements ($m^3\ ha^{-1}$) according to hydro-module zones and actual water application requirements in the Khorezm region, Uzbekistan.

Crop Type	Crop Water Requirement According to Hydro-Module Zone			Average	Actual Water Application Requirement
	VII	VIII	IX		
Cotton	6400	4900	5300	5533	8853
Wheat	4000	3200	3600	3600	5760
Rice	26,200	26,200	26,200	26,200	41,920
Other	5900	5200	5700	5600	8960

Note: Crop water requirements based on recommendations of [50,51]; irrigation network efficiency of 63% for Khorezm according to [15].

All hydro-module zones in Khorezm are typified by groundwater levels of 1–2 m below the soil surface [52]. The crop irrigation requirements were further adjusted for conveyance losses in irrigation canals by considering the overall irrigation network efficiency of 63% in Khorezm [15]. In SWAT, the actual amounts of irrigation water applied (considering the irrigation supply and irrigation losses) were assigned to different crops based on the local standards for crop irrigation.

The irrigation demand of trees, i.e., Russian olive (*Elaeagnus angustifolia* L.), Euphrates poplar (*Populus euphratica* Oliv.), and Siberian elm (*Ulmus pumila* L.) comprised less than 2000 m^3 ha^{-1} in the first two growing seasons based on field-scale (<2.5 ha) afforestation experiments on marginal cropland in Khorezm [53]. After the irrigation was discontinued, the tree plantations fully relied on shallow groundwater use until the cutting age [54]

2.3.5. Afforestation Scenarios

The delineation of the marginal cropland, which is characterized by sufficient surface water availability to satisfy the initial irrigation demand of tree plantations [15] defined the total cropland area of low productivity but suitable for afforestation. In total, 67% (approximately 663 km^2) of the marginal cropland (or 16.6% of the total area in Khorezm), mostly in the southwestern part of the region, was found to be suitable for conversion to tree plantations (Figure 7). Of these, "moderately marginal" croplands were dominant, followed by "slightly marginal," "marginal," and "highly marginal. These spatial data were integrated with land use maps of 2005 (representing average conditions) and 2008 (representing drought) (Figure 6a,d) considering the following afforestation scenarios:

1. "100% afforestation": Afforestation of the entire marginal cropland characterized by sufficient water availability for trees (67% of the total marginal cropland area, that is, approximately 663 km^2). The two related scenarios (LU2005-100% and LU2008-100%) are depicted in Figure 6c,f for average and drought years, respectively.
2. "62% afforestation": Afforestation of only "moderately marginal" and "marginal" cropland area with sufficient water availability for trees, comprising 62% of total marginal land, that is, approximately 408 km^2 (or 10.2% of Khorezm's area). The two related scenarios (LU2005-62% and LU2008-62%) are depicted in Figure 6b,e for average and drought years, respectively.

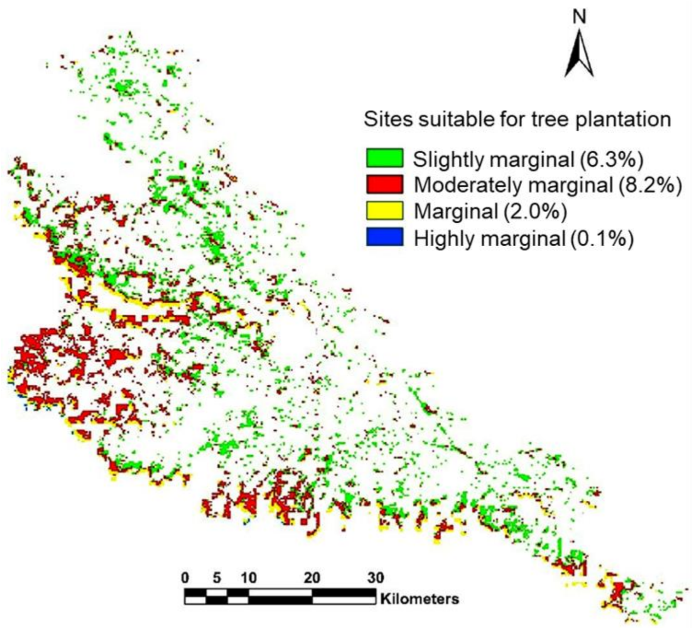

Figure 7. Marginal croplands with sufficient water availability for afforestation estimated based on land and water use data for 2003–2009. Source: [15].

These scenarios were used in the SWAT to assess the impact of afforestation on water balance components (Figures 2 and 7).

3. Results

3.1. Land Use Allocation under Simulation Scenarios

Land use statistics for the years 2005 and 2008 revealed the predominant share of total and marginal croplands growing cotton, followed by those containing wheat rotations with other crops in either year. Considering the land use changes in afforestation scenarios based on the land use map of 2005, the "100% afforestation" scenario would result in approximately 438 km^2 (10.8%) of (marginal) cotton land converted to tree plantation under average water availability conditions whereas only 263 km^2 (6.5%) of the land would be afforested in the "62% afforestation" scenario (Figure 8). Based on the land use map of 2008, the "100% afforestation" would result in approximately 234 km^2 (5.8%) of cotton land converted to tree plantations. In the "62% afforestation" scenario, this land use change would occur only on 119 km^2 (2.9%) of cotton land.

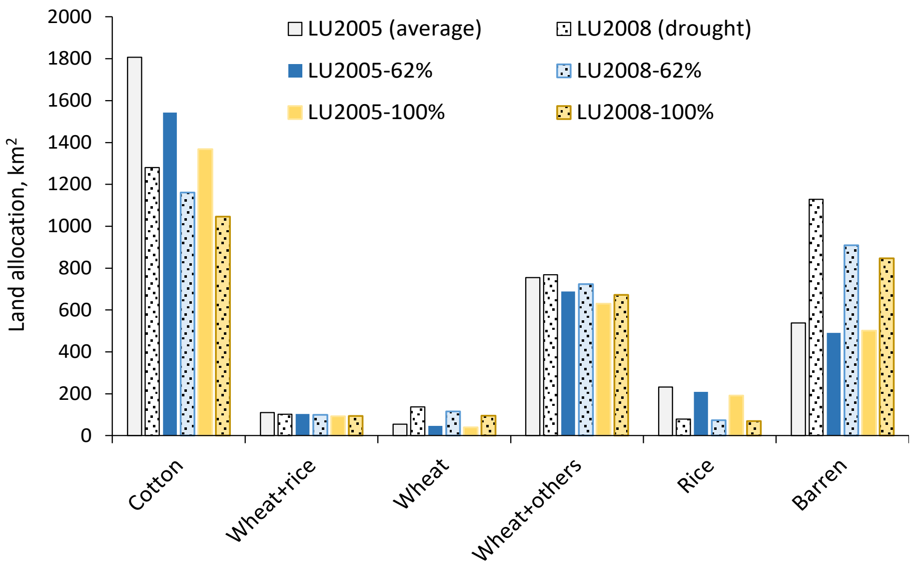

Figure 8. Shares of land use classes in the Khorezm region (Uzbekistan) in 2005 representing average climate conditions (LU2005), the 62% afforestation scenario (LU2005-62%), and the 100% afforestation scenario (LU2005-100%), land use in 2008 representing drought conditions (LU2008), the 62% afforestation scenario (LU2008-62%), and the 100% afforestation scenario (LU2008-100%).

The land use allocations from 2005 to 2008 indicate a significantly increased proportion of fallow land, approaching that of land cultivated with the predominant crop of cotton in 2008. Consequently, in this land use category, the afforested area increased from 1.1% and 0.9% in 2005 to 5.4% and 7.0% in 2008 in the 62% and 100% afforestation scenarios, respectively. The share of afforested cropland in addition to cotton land totaled 2.6% and 4.9% in 2005 and 1.9% and 3.9% in 2008 in the respective afforestation scenarios.

3.2. Impact of Afforestation on Water Balance Components

The SWAT-based simulations considering the average water availability conditions (land use map of 2005) showed declining values for all the examined water balance components, namely GWQ, percolation, soil moisture, water yields (surface runoff + groundwater lateral flow), and AET as a result of both the 62% and 100% afforestation for marginal croplands (Figure 9). The GWQ was reduced by 62 mm and 116 mm in the 62% and 100% afforestation scenarios, respectively, under average water availability conditions. Similarly, percolation was reduced by 67 mm and 126 mm, whereas soil moisture showed only a small decline. Notably, AET would also decrease by 64 mm in 100% afforestation.

The water yield was reduced by 66 mm and 124 mm in the 62% and 100% afforestation scenarios, respectively.

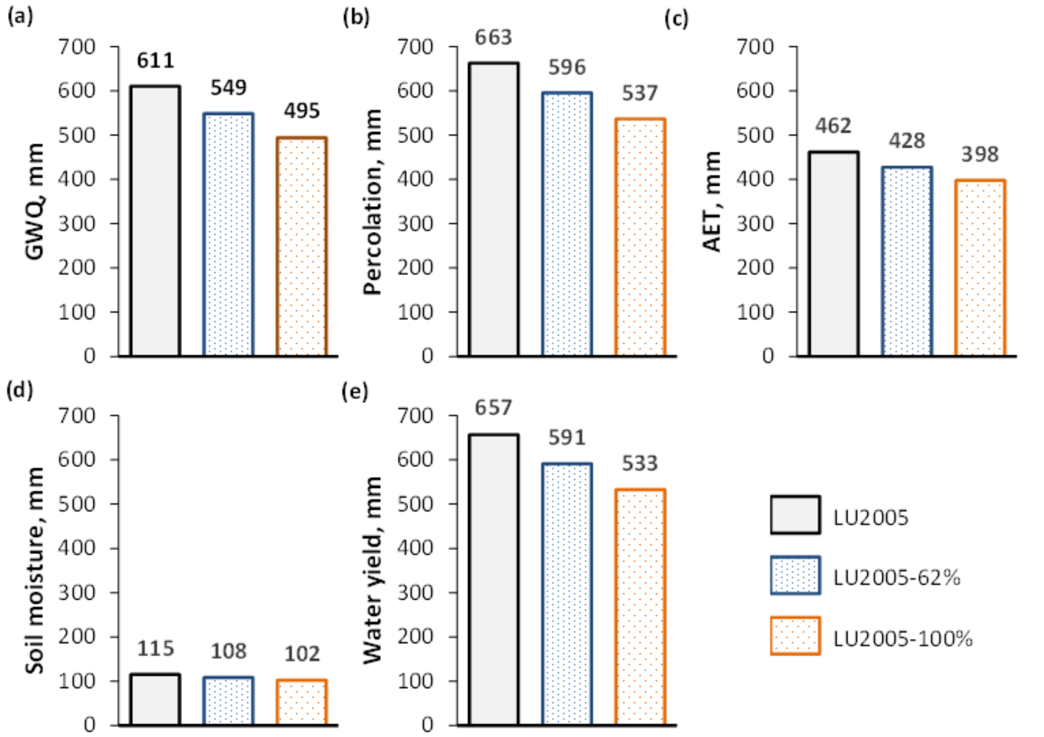

Figure 9. Water balance components: groundwater contribution to streamflow, GWQ (**a**), percolation (**b**), AET (**c**), soil moisture (**d**), and water yield (**e**) estimated for the observed land use pattern (LU2005) and under 62% (LU2005-62%) and 100% (LU2005-100%) afforestation scenarios in 2005, representing average conditions.

Under drought conditions, as reflected in the 2008 land use map, a similar declining trend was observed for all computed water balance components in either afforestation scenario for marginal land (Figure 10). However, with decreased water availability and a consequently reduced cropping area and crop water use, the reductions in water balance component values were also smaller. For example, in the 100% afforestation scenario within the land use map of 2008, the reduction in AET was approximately 19 mm less, and that the water yield was approximately 44 mm less than the simulated values in the 2005 land use map.

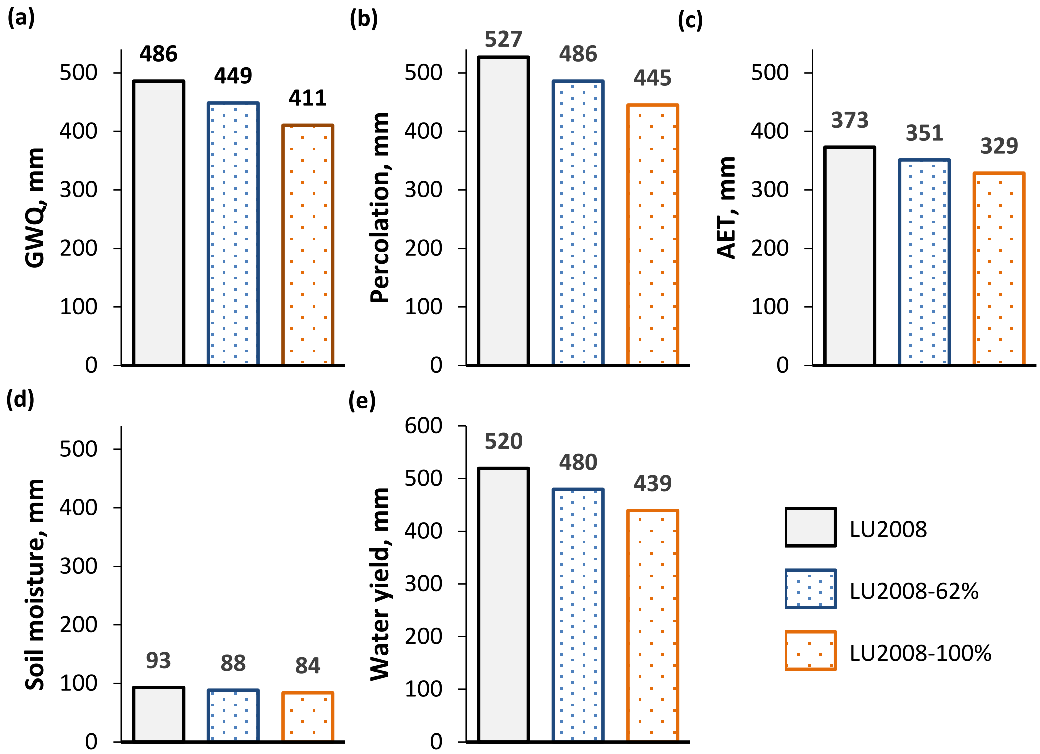

Figure 10. Water balance components: groundwater contribution to streamflow, GWQ (**a**), percolation (**b**), AET (**c**), soil moisture (**d**), and water yield (**e**) estimated for the observed land use pattern (LU2008) and under 62% (LU2008-62%) and 100% (LU2008-100%) afforestation scenarios in 2008, representing drought conditions.

3.3. Plausibility of the SWAT Simulation and Estimated Water Saving

A plausibility check of the SWAT simulations was conducted for 2005, representing an average water supply and demand. Relating the simulated annual water yield to the gross irrigation input plus precipitation (2663/(4741 + 450) in mln m^3) resulted in a drainage ratio of 51%. This value is somewhat lower than those based on the monitoring by [6,55]. However, reference [55] reported a drainage ratio of 58% for Khorezm, but only in the vegetation (thus only in the irrigated) period of 2005; Reference [6] reported a ratio of 55% for the Water Consumers Association Shomokhulun in the vegetation period of 2007.

In the estimation of water-saving potential from replacing crops on marginal land with trees, we considered (i) the LU2005-100% scenario, that is, the change in cropping pattern in 2005 following the afforestation of all marginal land (approximately 663 km^2; Figure 8), (ii) the gross irrigation water input based on the crop-specific norms stated in Table 1, (iii) the water amount for pre-seasonal salt leaching reported by [41,42], that is, 500 mm for cotton, 300 mm for rice, 250 mm for wheat, and 200 mm for wheat + other, and (iv) the network efficiency of 63% [15]. The estimated reduction in gross irrigation water input amounts to 1037 mln m^3 and is the approximation for the water-saving potential. This amount equals approximately 22% of the water withdrawal for irrigation in Khorezm from the Amudarya River (approximately 4741 mln m^3 in 2005).

Furthermore, the SWAT-simulated water yield of 657 mm (Figure 9e) approximated the total drainage flow and was equal to a discharge sum of 2663 mln m^3 in 2005. As simulated by SWAT in the LU2005-100% scenario, this drainage output can be lowered to 2159 mln m^3 (533 mm; Figure 9e) because of the reduced irrigation water input following afforestation.

4. Discussion

4.1. Limitations of SWAT-Based Analysis

Simulations based on SWAT modeling allowed for evaluating the alternative conception of land and water use at a regional scale because an analysis of the monitored data alone could not include the effect of planned strategies. The major limitation of this study is the lack of observed catchment discharge data to ensure the adequate calibration and validation of SWAT. However, we parameterized the crop and soil input data using values specific to the study area. The SWAT-computed water balance components based on land and water use in 2005, the year representing average conditions, showed a close agreement with the observed values available for Khorezm. Specifically, the drainage ratio integrating both the water yield (mainly as drainage output) and water supply (irrigation water input and precipitation) at the regional scale was matched by the SWAT simulations. This indicates the overall plausibility of the model application. The modeled PET value (1269 mm) falls within the previously reported range of 1150–1500 mm in agricultural Khorezm [40,56]. The SWAT-computed AET value (462 mm) was lower than the remote sensing-based estimate of seasonal AET (March to October) averaging 627 mm during 2003–2011 for Khorezm [57]). The other water balance components, besides soil moisture (highly variable under irrigated conditions), have not been previously reported for Khorezm, thereby precluding comparisons with the modeled data; these are therefore the first and only available estimates to date.

Another major limitation of our analysis is the lack of elaborate groundwater modeling. The groundwater contribution is roughly accounted for in the recommended irrigation norms for the hydro-module zone; groundwater also constitutes the main source of water by tree plantations introduced on marginal land. In this view, the groundwater component is important in simulating the impact of afforestation on water balance; however, it is currently not comprehensively developed in SWAT. For each HRU, the aquifer system is only represented by two layers: shallow/unconfined and deep/confined aquifers, and a linear reservoir model is used to simulate the groundwater flow. The water from the shallow aquifer could move to the deep aquifer, whereas the reverse process was not allowed, which may lead to inaccuracies in simulations for the areas where the groundwater system is more complicated and the drainage basin is predominately recharged by groundwater [58].

4.2. Impact of Afforestation on Irrigation Water Savings and Drainage

Forests and trees are important modulators of global, regional, and local hydrological cycles and patterns [22,59,60]. Negative hydrological impacts, such as the depletion of soil water and reduced annual runoff and water yields, are often observed for dryland afforestation [18,20,24], especially in large-scale planting schemes [19,61]. However, with the excessive cropland irrigation in Khorezm [5]), the reduction in all examined water balance components following the afforestation of marginal land reflects the reduced irrigation inputs and lowered drainage output. These impacts have positive implications for irrigation water saving [62] and mitigation of elevated groundwater tables [16,17]. Water-saving strategies are essential for irrigated areas in the downstream countries of Central Asia where the water consumption rates are among the highest worldwide and both irrigation water-use efficiency and water productivity remain low [9]. Converting marginal cropland, which is otherwise cultivated with low-yielding and water-consumptive crops, to tree plantations [13], offers advantages for sustaining long-term irrigated crop production. This outcome is particularly desirable as climate change increases precarity to water supplies [1,2] and sharpens competition for water in the transboundary Amudarya Basin [9].

The magnitude of reduction in water balance component values (although favorable for reducing the irrigation water losses in the region) is not likely to cause dramatic declines in soil moisture and the groundwater level, which would have jeopardized the sustainability of crop and tree water use within the study region. Even in the larger-scale afforestation scenario (LU2005-100%), only approximately 11% of cotton-cropped land can be converted to tree plantations. This land use conversion would result in financial gains considering the low yields of common crops versus the high production value of trees on marginal land, as well as the possibility of utilizing water savings from the afforestation for the cultivation of alternative, commercially attractive crops on productive cropland [13]. In Central Asia, afforestation of degraded croplands could increase low forest cover, especially in downstream areas dominated by annual crops [63], while not competing for crop production on prime farming land.

In other irrigated drylands experiencing soil salinization, such as in India and Australia, reducing annual runoff and enhancing AET via tree planting (bio-drainage) has been a deliberate strategy for controlling elevated groundwater tables and soil salinization [16,17]. To ensure effective salinity control, this bio-drainage option requires the strategic placement of trees within the landscape (possibly in combination with conventional drainage facilities), which is not consistent with the criteria used for spatial targeting of afforestation on marginal land [11,15]. In addition, according to the SWAT simulations, the AET decreased in all afforestation scenarios, in contrast to the more common expectation from trees to enhance evapotranspiration (e.g., [23]. A reduced AET can be viewed as a desirable outcome of afforestation in adaptation to climate change-induced drought events (LU2008 scenario), but it might limit the bio-drainage capacity. Overall, even if reductions in soil salinity through afforestation might not be expected in the study region, the increased productivity of marginal cropland planted with salt-tolerant tree species capable of utilizing relatively untapped groundwater resources is still a viable option for managing salinized croplands.

5. Conclusions

The SWAT modeling results indicated a dramatic decrease in the examined water balance components (i.e., GWQ, percolation, AET, soil moisture, and water yield) in afforestation scenarios considering both low and average water availability for irrigation. The decrease would largely be caused by the reduced irrigation demand of trees as opposed to the main crop of cotton. These findings support the hydrological feasibility of afforestation at a regional scale, that is, on 100% of marginal cropland (approximately 663 km^2) in the study region. Moreover, conversion of degraded cropland characterized by over-irrigation and shallow groundwater tables to a tree plantation may contribute to a portfolio of water-saving options to reduce Amudarya water withdrawals and improve the efficiency of water and land use in the lower reaches. Further modeling analysis must integrate the dynamics of groundwater components in the assessment of long-term hydrological impacts of afforestation.

Supplementary Materials: The following are available online at https://www.mdpi.com/article/10.3390/w13101433/s1, Figure S1: SWAT-delineated 107 sub-basins in the study region of Khorezm, Uzbekistan; Table S1: Input data used in SWAT model for estimation of water balance components.

Author Contributions: Conceptualization, N.K. and A.K.; methodology, N.K., A.K., B.T.; modeling analysis, N.K.; data curation, A.K., P.K., and J.P.A.L.; writing—original draft preparation, N.K. and A.K.; writing—review and editing, all authors; project administration, A.K.; funding acquisition, A.K. All authors have read and agreed to the published version of the manuscript.

Funding: This research was funded by the National Research Foundation of Korea (NRF), grant number 2018K1A3A7A03089842 and EU 2020 Horizon, grant number 776019.

Institutional Review Board Statement: Not applicable.

Informed Consent Statement: Not applicable.

Data Availability Statement: The data presented in this study are available on request from the authors.

Acknowledgments: The support of the Open Interoperable Platform for Unified Access and Analysis of Earth Observation Data (776019-EOPEN-H2020-EO-2017/H2020-EO-2017) project is gratefully acknowledged.

Conflicts of Interest: The authors declare no conflict of interest.

References

1. World Bank. *Climate Change in Central Asia, Illustrated Summary*; World Bank: Washington, DC, USA, 2020.
2. Punkari, M.; Droogers, P.; Immerzeel, W.; Korhonen, N.; Lutz, A.; Venäläinen, A. *Climate Change and Sustainable Water Management in Central Asia Central and West Asia Working Paper Series*; Asian Development Bank: Mandaluyong, Metro Manila, Philippines, 2014.
3. Parry, M.L.; Canziani, O.F.; Palutikof, J.P.; van der Linden, P.J.; Hanson, C.E. *Climate Change 2007: Impacts, Adaptation and Vulnerability*; Cambridge University Press: Cambridge, UK; New York, NY, USA, 2007; p. 976.
4. Roll, G.; Alexeeva, N.; Aladin, N.; Plotnikov, I.; Sokolov, V.; Sarsembekov, T.; Micklin, P. Aral Sea: Experiences and Lessons Learned Brief. Lake Basin Management Initiative. 2005. Available online: https://www.iwlearn.net/documents/6014 (accessed on 20 May 2021).
5. Awan, U.K.; Ibrakhimov, M.; Tischbein, B.; Kamalov, P.; Martius, C.; Lamers, J.P.A. Improving Irrigation Water Operation in the Lower Reaches of the Amu Darya River—Current Status and Suggestions. *Irrig. Drain.* **2011**, *60*, 600–612. [CrossRef]
6. Awan, U.K.; Tischbein, B.; Conrad, C.; Martius, C.; Hafeez, M. Remote Sensing and Hydrological Measurements for Irrigation Performance Assessments in a Water User Association in the Lower Amu Darya River Basin. *Water Resour. Manag.* **2011**, *25*, 2467–2485. [CrossRef]
7. Dukhovny, V.; Yakubov, K.; Usmano, A.; Yakubov, M. Drainage water management in the Aral Sea Basin. In *Agricultural Drainage Water Management in Arid and Semi-Arid Areas. FAO Irrigation and Drainage Paper*; World Food Organization: Rome, Italy, 2002; Volume 61, pp. 1–23.
8. Saigal, S. *Issues and Approaches to Combat Desertification*; Asian Development Bank: Tashkent, Uzbekistan, 2003; p. 51.
9. Varis, O. Resources: Curb vast water use in central Asia. *Nature* **2014**, *514*, 27–29. [CrossRef] [PubMed]
10. Djalilov, B.M.; Khamzina, A.; Hornidge, A.-K.; Lamers, J.P. Exploring constraints and incentives for the adoption of agroforestry practices on degraded cropland in Uzbekistan. *J. Environ. Plan. Manag.* **2016**, *59*, 142–162. [CrossRef]
11. Dubovyk, O.; Menz, G.; Khamzina, A. Land suitability assessment for afforestation with Elaeagnus angustifolia L. in degraded agricultural areas of the lower Amu Darya River Basin. *Land Degrad. Dev.* **2016**, *27*, 1831–1839. [CrossRef]
12. Khamzina, A.; Lamers, J.P.A.; Vlek, P.L.G. Conversion of degraded cropland to tree plantations for ecosystem and livelihood benefits. In *Cotton, Water, Salts and Soums*; Martius, C., Rudenko, I., Lamers, J.P.A., Vlek, P.L.G., Eds.; Springer: Berlin/Heidelberg, Germany, 2012; pp. 235–248. [CrossRef]
13. Djanibekov, U.; Khamzina, A. Stochastic Economic Assessment of Afforestation on Marginal Land in Irrigated Farming System. *Environ. Resour. Econ.* **2016**, *63*, 95–117. [CrossRef]
14. Khamzina, A.; Lamers, J.P.A.; Vlek, P.L.G. Tree establishment under deficit irrigation on degraded agricultural land in the lower Amu Darya River region, Aral Sea Basin. *For. Ecol. Manag.* **2008**, *255*, 168–178. [CrossRef]
15. Kumar, N.; Khamzina, A.; Tischbein, B.; Knöfel, P.; Conrad, C.; Lamers, J.P.A. Spatio-temporal supply–demand of surface water for agroforestry planning in saline landscape of the lower Amudarya Basin. *J. Arid Environ.* **2019**, *162*, 53–61. [CrossRef]
16. Dagar, J.C.; Gupta, S.R. Agroforestry Interventions for Rehabilitating Salt-Affected and Waterlogged Marginal Landscapes. In *Agroforestry for Degraded Landscapes*; Springer: Singapore, 2020; pp. 111–162. [CrossRef]
17. Minhas, P.S.; Yadav, R.K.; Bali, A. Perspectives on reviving waterlogged and saline soils through plantation forestry. *Agric. Water Manag.* **2020**, *232*, 106063. [CrossRef]
18. Cao, S.; Chen, L.; Shankman, D.; Wang, C.; Wang, X.; Zhang, H. Excessive reliance on afforestation in China's arid and semi-arid regions: Lessons in ecological restoration. *Earth-Sci. Rev.* **2011**, *104*, 240–245. [CrossRef]
19. Hübner, L. Large Scale Afforestation in Arid and Semi-Arid Climate: Hydrologic-Ecological Lessons Learned and Concept of Modular Hydrologic Connectivity of Vegetation. *J. Agric. Food Dev.* **2020**, *6*, 10–21. [CrossRef]
20. Sun, G.; Zhou, G.; Zhang, Z.; Wei, X.; McNulty, S.G.; Vose, J.M. Potential water yield reduction due to forestation across China. *J. Hydrol.* **2006**, *328*, 548–558. [CrossRef]
21. Farley, K.A.; Jobbágy, E.G.; Jackson, R.B. Effects of afforestation on water yield: A global synthesis with implications for policy. *Glob. Chang. Biol.* **2005**, *11*, 1565–1576. [CrossRef]
22. Filoso, S.; Bezerra, M.O.; Weiss, K.C.; Palmer, M.A. Impacts of forest restoration on water yield: A systematic review. *PLoS ONE* **2017**, *12*, e0183210. [CrossRef] [PubMed]
23. Jackson, R.B.; Jobbágy, E.G.; Avissar, R.; Roy, S.B.; Barrett, D.J.; Cook, C.W.; Farley, K.A.; Le Maitre, D.C.; McCarl, B.A.; Murray, B.C. Trading water for carbon with biological carbon sequestration. *Science* **2005**, *310*, 1944–1947. [CrossRef]
24. Milkovic, M.; Paruelo, J.M.; Nosetto, M.D. Hydrological impacts of afforestation in the semiarid Patagonia: A modelling approach. *Ecohydrology* **2019**, *12*, 2113. [CrossRef]
25. Konikow, L.F.; Reilly, T.E. Ground-water Modelling. In *The Handbook of Groundwater Engineering*; Delleur, J.W., Ed.; CRC Press: Boca Raton, FL, USA, 1998; pp. 1–20.
26. Bergström, S.; Forsman, A. Development of a conceptual deterministic rainfall-runoff mode. *Nord. Hydrol.* **1973**, *4*, 240–253. [CrossRef]
27. Im, S.; Kim, H.; Kim, C.; Jang, C. Assessing the impacts of land use changes on watershed hydrology using MIKE SHE. *Environ. Geol.* **2009**, *57*, 231. [CrossRef]

28. Refshaard, J.C.; Storm, B. MIKE SHE. In *Computer Models of Watershed Hydrology*; Water Resources Publications: Colorado, CO, USA, 1995; pp. 809–846.
29. Niehoff, D.; Fritsch, U.; Bronstert, A. Land-use impacts on storm-runoff generation: Scenarios of land-use change and simulation of hydrological response in a meso-scale catchment in SW-Germany. *J. Hydrol.* **2002**, *267*, 80–93. [CrossRef]
30. Schulla, J. Hydrologische Modellierung von Flußeinzugsgebieten zur Abschätzung der Folgen von Klimaänderungen (Hydrological modelling of river basins for evaluating the impacts of climatic changes). *Züricher Geogr. Hefte*. 1997. Available online: https://doi.org/10.3929/ethz-a-001763261 (accessed on 20 May 2021).
31. Srivastava, A.; Kumari, N.; Maza, M. Hydrological Response to Agricultural Land Use Heterogeneity Using Variable Infiltration Capacity Model. *Water Resour. Manag.* **2020**, *34*, 3779–3794. [CrossRef]
32. Arnold, J.G.; Srinivasan, R.; Muttiah, R.S.; Williams, J.R. Large area hydrologic modeling and assessment part I: Model development. *J. Am. Water Resour. Assoc.* **1998**, *34*, 73–89. [CrossRef]
33. Fohrer, N.; Haverkamp, S.; Eckhardt, K.; Frede, H.-G. Hydrologic response to land use changes on the catchment scale. *Phys. Chem. Earth Part B Hydrol. Ocean. Atmos.* **2001**, *26*, 577–582. [CrossRef]
34. Durło, G.; Jagiełło-Leńczuk, K.; Małek, S.; Banach, J.; Dudek, K.; Kormanek, M. Hydrological responses to forest cover change in mountains under projected climate conditions. *Int. J. Environ. Agric. Res.* **2016**, *2*, 60–68.
35. Kim, G.S.; Lim, C.-H.; Kim, S.J.; Lee, J.; Son, Y.; Lee, W.-K. Effect of national-scale afforestation on forest water supply and soil loss in South Korea, 1971–2010. *Sustainability* **2017**, *9*, 1017. [CrossRef]
36. Von Stackelberg, N.O.; Chescheir, G.M.; Skaggs, R.W.; Amatya, D.M. Simulation of the hydrologic effects of afforestation in the Tacuarembó River Basin, Uruguay. *Trans. ASABE* **2007**, *50*, 455–468. [CrossRef]
37. Gassman, P.W.; Reyes, M.R.; Green, C.H.; Arnold, J.G. The soil and water assessment tool: Historical development, applications, and future research directions. *Trans. ASABE* **2007**, *50*, 1211–1250. [CrossRef]
38. Douglas-Mankin, K.; Srinivasan, R.; Arnold, J. Soil and Water Assessment Tool (SWAT) model: Current developments and applications. *Trans. ASABE* **2010**, *53*, 1423–1431. [CrossRef]
39. Ibrakhimov, M.; Khamzina, A.; Forkutsa, I.; Paluasheva, G.; Lamers, J.P.A.; Tischbein, B.; Vlek, P.L.G.; Martius, C. Groundwater table and salinity: Spatial and temporal distribution and influence on soil salinization in Khorezm region (Uzbekistan, Aral Sea Basin). *Irrig. Drain. Syst.* **2007**, *21*, 219–236. [CrossRef]
40. Ibrakhimov, M.; Martius, C.; Lamers, J.P.A.; Tischbein, B. The dynamics of groundwater table and salinity over 17 years in Khorezm. *Agric. Water Manag.* **2011**, *101*, 52–61. [CrossRef]
41. Akramkhanov, A.; Tischbein, B.; Awan, U.K. Effective management of soil salinity—Revising leaching norms. In *Technologies, Policies and Practices for the Lower Amudarya Region*; Lamers, J.P.A., Khamzina, A., Rudenko, I., Vlek, P.L.G., Eds.; V&R Unipress, Bonn University Press: Göttingen, Germany, 2014; pp. 121–134. ISBN 978-3-8471-0297-7.
42. Forkutsa, I.; Sommer, R.; Shirokova, Y.I.; Lamers, J.P.A.; Kienzler, K.; Tischbein, B.; Martius, C.; Vlek, P.L.G. Modeling irrigated cotton with shallow groundwater in the Aral Sea Basin of Uzbekistan: II. Soil salinity dynamics. *Irrig. Sci.* **2009**, *27*, 319–330. [CrossRef]
43. Consultative Group for International Agricultural Research (CGIAR). SRTM 90m DEM Digital Elevation Database. Available online: https://srtm.csi.cgiar.org/ (accessed on 10 May 2021).
44. Conrad, C.; Schorcht, G.; Tischbein, B.; Davletov, S.; Sultonov, M.; Lamers, J.P.A. Agro-meteorological trends of recent climate development in Khorezm and implications for crop production. In *Cotton, Water, Salts and Soums*; Martius, C., Rudenko, I., Lamers, J.P.A., Vlek, P.L.G., Eds.; Springer: Berlin/Heidelberg, Germany, 2012; pp. 25–36. [CrossRef]
45. Lamers, J.P.A.; Khamzina, A.; Rudenko, I.; Vlek, P.L. *Restructuring Land Allocation, Water Use and Agricultural Value Chains: Technologies, Policies and Practices for the Lower Amudarya Region*; V&R Unipress, Bonn University Press: Göttingen, Germany, 2014; ISBN 978-3-8471-0297-7.
46. Uzgipromeliovodkhoz Institute. *Soil Types by Rayon in Khorezm Region*; OOO UZGIP: Tashkent, Uzbekistan, 1999.
47. U.S. Department of Agriculture, Natural Resources Conservation Service. *National Soil Survey Handbook*; 1996. Available online: http://www.nrcs.usda.gov/wps/portal/nrcs/detail/soils/ref/?cid=nrcs142p2_054242 (accessed on 20 May 2021).
48. Williams, J.R. The EPIC model. In *Computer Models of Watershed Hydrology*; Water Resources Publications: Colorado, CO, USA, 1995; pp. 909–1000.
49. Conrad, C.; Lamers, J.P.A.; Ibragimov, N.; Löw, F.; Martius, C. Analysing irrigated crop rotation patterns in arid Uzbekistan by the means of remote sensing: A case study on post-Soviet agricultural land use. *J. Arid Environ.* **2016**, *124*, 150–159. [CrossRef]
50. UzNIIKh. (Uzbekistan Science and Research Institute of Cotton Culture). In *Hydro-Module Zoning and Irrigation Regimes of Agricultural Crops for Administrative Regions of Uzbekistan*; UzNIIKh: Tashkent, Uzbekistan, 1992.
51. Ministry of Agriculture and Water Resources of Uzbekistan (MAWR). *Guide for Water Engineers in Shirkats and WUAs*; Ministry of Agriculture and Water Resources of Uzbekistan (MAWR): Tashkent, Uzbekistan, 2001.
52. OblVvodKkhoz (Department of Agriculture and Water Resources in Khorezm Region). *Hydro-Module-Zones in Khorezm for 2002*; OblVodKhoz: Khorezm, Uzbekistan, 2004.
53. Khamzina, A. The Assessment of Tree Species and Irrigation Techniques for Afforestation of Degraded Agricultural Landscapes in Khorezm, Uzbekistan, Aral Sea Basin. Ph.D. Thesis, Center for Development Research (ZEF), University of Bonn, Cuvillier Verlag, Göttingen, Germany, 2006.

54. Khamzina, A.; Lamers, J.P.A.; Martius, C. Above-and belowground litter stocks and decay at a multi-species afforestation site on arid, saline soil. *Nutr. Cycl. Agroecosyst.* **2016**, *104*, 187–199. [CrossRef]
55. Conrad, C.; Dech, S.W.; Hafeez, M.; Lamers, J.P.A.; Tischbein, B. Remote sensing and hydrological measurement based irrigation performance assessments in the upper Amu Darya Delta, Central Asia. *Phys. Chem. Earth* **2013**, *61*, 52–62. [CrossRef]
56. Tischbein, B.; Manschadi, A.M.; Hornidge, A.-K.; Conrad, C.; Lamers, J.P.; Oberkircher, L.; Schorcht, G.; Vlek, P.L. Ansätze für eine effizientere Wassernutzung in der Provinz Khorezm, Usbekistan. *Hydrol. Und Wasserbewirtsch.* **2011**, *55*, 116–125.
57. Knöfel, P. Optimization of Energy Balance Modelling in Order to Determine Evapotranspiration by Developing a Physical Based Soil Heat Flux Approach on the Example of Khorezm Region in Uzbekistan. Ph.D. Thesis, University of Würzburg, Würzburg, Germany, 2016.
58. Shao, G.; Zhang, D.; Guan, Y.; Xie, Y.; Huang, F. Application of SWAT model with a modified groundwater module to the semi-arid Hailiutu River Catchment, Northwest China. *Sustainability* **2019**, *11*, 2031. [CrossRef]
59. Ellison, D.; Futter, N.M.; Bishop, K. On the forest cover–water yield debate: From demand-to supply-side thinking. *Glob. Chang. Biol.* **2012**, *18*, 806–820. [CrossRef]
60. Mátyás, C.; Sun, G. Forests in a water limited world under climate change. *Environ. Res. Lett.* **2014**, *9*, 085001. [CrossRef]
61. Cao, S.; Wang, G.; Chen, L. Questionable value of planting thirsty trees in dry regions. *Nature* **2010**, *465*, 31. [CrossRef]
62. Bekchanov, M.; Lamers, J.P.A.; Martius, C. Pros and cons of adopting water-wise approaches in the lower reaches of the Amu Darya: A socio-economic view. *Water* **2010**, *2*, 200–216. [CrossRef]
63. Yin, H.; Khamzina, A.; Pflugmacher, D.; Martius, C. Forest cover mapping in post-Soviet Central Asia using multi-resolution remote sensing imagery. *Sci. Rep.* **2017**, *7*, 1–11. [CrossRef]